

# Parameterization of an irregular-shaped ice particle model in climate simulations with community atmospheric model version5

Ming Li (1), Husi Letu\* (1,2), Yiran Peng (3), Hiroshi Ishimoto (4), Yanluan Lin (3), Takashi Y. Nakajima (2), Anthony Baran (5), Jiancheng Shi (1)

1 Aerospace Information Research Institute, Chinese Academy of Sciences, Beijing 100010, China;

2 Research and Information Center (TRIC), Tokai University, 4-1-1 Kitakaname Hiratsuka, Kanagawa 259-1292, Japan

3 Department of Earth Science System, Tsinghua University, Beijing 10084, China

4 Meteorological Research Institute, Japan Meteorological Agency (JMA), Nagamine 1-1, Tsukuba 305-0052, Japan.

5 Met Office, Fitzroy Road, Exeter EX1 3PB, UK

**KEY WORDS:** irregular-shaped ice particle, ice cloud parameterization, optical properties, radiative properties

**ABSTRACT:** Ice cloud microphysical properties such as ice particle habits and their single-scattering properties are the main influencing factors of ice cloud radiative properties. This paper developed a new ice cloud parameterization (called “Voronoi scheme”) based on an complex and highly irregular-shaped ice particle habit called Voronoi aggregate. First, bulk optical properties fitting formula as function of the effective particle radius of ice cloud at given narrowband are calculated with scattering properties databases of Voronoi ice particle and particle size distributions of 11 field campaigns. Then, broadband-averaged bulk scattering and absorption properties of ice cloud are integrated over set band limits of the Rapid Radiative Transfer Model (RRTMG) and the Community Atmospheric Model Version 5 (CAM5). Finally, The influence of Voronoi ice particle on the ice cloud radiative effect are compared with four existing schemes (Fu scheme, Baum-Yang scheme, Mitchell scheme and Yi scheme), and validated against satellite observations. The CAM5 simulation results show that the differences in TOA cloud radiative forcing (CRF) for new parameterization are in the range of 1.2-5.6 W/m<sup>2</sup>, which is lower than Mitchell scheme. In general, the new parameterization low the discrepancy between simulated 10-yr mean TOA SW and LW cloud radiative forcing (CRF) and observation mean values.

## 1. Introduction

Single scattering properties of ice particle model and ice cloud parameterization are important for remote sensing application and climate model simulations of ice cloud radiative properties. Ice cloud parameterization accuracy is mainly determined by the single scattering properties of ice particle model. Many ice cloud parameterization schemes have been developed for ice cloud remote sensing and climate model simulations. Fu and Liou (1993) (referred to as “Fu Scheme”) applied the hexagonal scheme to the four-stream scheme of Fu-Liou radiative transfer model (Fu, 1996). Nine ice crystal habits from a library of Yang et al (2013) are utilized to develop a parametrization scheme (referred to as “BY Scheme”) and applied it to the development of ice cloud products in MODIS Collection 5. Yi et al (2013) developed the parametrizations (referred to as “Yi Scheme”) based on a general habit mixture

model that includes nine pristine habits of varying roughness. In the Community Earth System Model, version1 (CESM1), the atmosphere component is the Community Atmosphere Model, Version 5 (CAM5). In CAM5, ice optical parameterization employs ice cloud parameterization developed by Mitchell et al, (1996, 2006) (hereafter called “Mitchell scheme”).

Optimal choice of ice particle habit is in demand to develop the ice cloud scheme as accurate as possible. Voronoi ice particel model has been utilized in the Global Change Observation Mission — Climate (GCOM-C), Himawari-8 and EarthCARE (Letu et al., 2016; Nakajima et al. 2019) satellite missions and has been proved to be efficient in remote sensing retrieval of ice cloud products. However, ice cloud modeling capabilities of Voronoi ice particle model is still unknown in global climate model (GCM) and lack of studies. As a further work of Letu et al, (2016), this study is aimed to improve an ice cloud scheme (hereafter called “Voronoi scheme”) based on Voronoi ice particle model in GCM and evaluate the capabilities of describing ice cloud radiative properties. Current work is presented as follows. Section 2 is the introduction of the study. Section 3 generally introduce the Voronoi single scattering properties from Voronoi databases, radiative transfer model RRTMG\_SW and GCM CAM used in this study, methods to calculate bulk optical properties, to develop an ice scheme based on Voronoi model. Bulk optical properties, RTM flux results and GCM CAM simulation results are given in Section 3. Section 4 is the conclusion of this study.

## 2. Single scattering properties of Voronoi model

In this study, we assume ice particle model as Voronoi model and utilized the single scattering properties (mainly including extinction efficiency ( $Q_{ext}$ ), single scattering albedo ( $Q_s$ ), absorption efficiency ( $Q_a$ ), asymmetry factor ( $g$ ) and scattering phase function) from the ultraviolet to the far IR of the Voronoi ice particle single-scattering-property database provided by Ishimoto et al, (2012) and Letu et al, (2016). Our study is to assess the ice cloud modeling capabilities of Vornoi model in the climate model simulations and quantify resulting radiative difference and mechanisms as the Voronoi model effects.

## 3. Methodology

### 3.1. Parameterization of ice cloud properties

The primary framework of ice cloud parameterization is as following steps: first, we used 14408 groups of microphysical data derived from aircraft field campaigns from Heymsfield et al (2013) to determine particle size distributions (PSDs) assumptions using gamma distribution (Mitchell et al., 1996) (equation (1-2)). Second, based on Voronoi single-scattering properties, we determined the effective particle diameter  $D_e$  and the ice cloud bulk scattering properties, including volumn-averaged extinction coefficient, single-scattering albedo and asymmetry factor for all given PSDs via equation (3-6). Third, we determine the coefficients of the polynomial expressions of ice cloud bulk scattering properties as functions of  $D_e$  at each wavelength.

$$n(D) = N_0 e^{-\lambda D}, D < 100 \mu m, \quad (1)$$

$$n(D) = N_0 D^\mu e^{-\lambda D}, D > 100 \mu m, \quad (2)$$

$$D_e = \frac{\sqrt{3} \int_{\lambda_{\min}}^{\lambda_{\max}} \int_{D_{\min}}^{D_{\max}} V(D)n(D)dD}{2 \int_{\lambda_{\min}}^{\lambda_{\max}} \int_{D_{\min}}^{D_{\max}} A(D)n(D)dD}, \beta = \frac{\int_{\lambda_{\min}}^{\lambda_{\max}} \int_{D_{\min}}^{D_{\max}} \sigma_{\text{ext}}(D)n(D)dD}{\rho_{\text{ice}} * \int_{\lambda_{\min}}^{\lambda_{\max}} \int_{D_{\min}}^{D_{\max}} V(D)n(D)dD}, \quad (3-4)$$

$$1-\varpi = \frac{\int_{\lambda_{\min}}^{\lambda_{\max}} \int_{D_{\min}}^{D_{\max}} \sigma_a(D)n(D)dD}{\int_{\lambda_{\min}}^{\lambda_{\max}} \int_{D_{\min}}^{D_{\max}} \sigma_{\text{ext}}(D)n(D)dD}, g = \frac{\int_{\lambda_{\min}}^{\lambda_{\max}} \int_{L_{\min}}^{L_{\max}} g(L)\sigma_{\text{sca}}(L)n(L)dL}{\int_{\lambda_{\min}}^{\lambda_{\max}} \int_{L_{\min}}^{L_{\max}} \sigma_{\text{sca}}(L)n(L)dL}, \quad (5-6)$$

### 3.2. Model simulation setting and validation data

To clarify radiative effects result from Voronoi scheme, we utilize radiative transfer model RRTMG (available from <http://rtweb.aer.com>) to calculate upward flux and downward flux and heating rate for Voronoi scheme and Mitchell scheme as comparison. Voronoi scheme and Mitchell scheme are implemented in CESM1 CAM5 for the comparison of ice cloud radiative forcing (CRF). CRF are calculated by downward flux and upward flux ( $\text{CRF} = N * (F_{\text{cloudy}} - F_{\text{clear}})$ ), where  $F_{\text{cloudy}}$  and  $F_{\text{clear}}$  are the net fluxes (downward minus upward) for cloudy (overcast) sky and clear sky, respectively, and  $N$  is cloud fraction.

## 4. Results and Discussion

### 4.1. Bulk optical properties

Bulk optical properties of Voronoi scheme are compared with that of Mitchell scheme in Fig. 4 for shortwave/longwave bands in RRTMG. Two schemes all show that ice particles  $D_e$  smaller than  $20\mu\text{m}$  have consistently high  $\beta$  at three wavelength, and  $\beta$  decrease abruptly with the increasing  $D_e$  from  $20\mu\text{m}$  to  $120\mu\text{m}$ . The  $\varpi$  approaches 1 and insensitive to  $D_e$  at visible and NIR-infrared spectrum for Voronoi scheme, this is mainly because the imaginary part of the refractive index of ice is close to 0. For Voronoi scheme, the asymmetry factor increase with the growing ice particle effective dimension at mid-infrared spectrum. Overall, differences between this two schemes hence originally root from different ice particle habits and the single scattering properties of ice particle model.

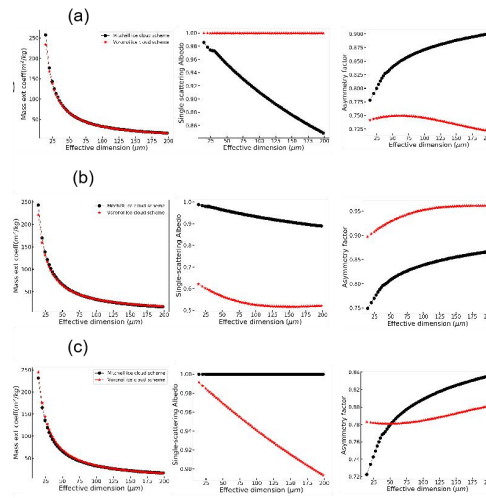


Figure 4. Bulk optical properties as functions of  $D_e$ . (a) is for band 3 (2.15–2.5 $\mu\text{m}$ ), (b) is for Band 6 (1.3–1.63 $\mu\text{m}$ ), (c) is for Band 10 (0.44–0.63 $\mu\text{m}$ ).

### 4.2. RTM model results

Based on the parametrization of session 2, the impacts of the Voronoi scheme and Mitchell scheme on the ice cloud radiative properties can be further discussed in a simplified atmospheric condition in the RRTMG. In this study, we select tropical atmospheric profile, in which tropical cirrus cloud is prescribed between 133.1 and 228.4 hPa, with ice particle effective dimension equal to  $40\mu\text{m}$  and ice water path equal to  $50\text{g m}^{-2}$ . According to Figure 4, we choose three spectrum in RRTMG\_SW, (a) band 3 ( $2.15 - 2.5\mu\text{m}$ ), (b) band 6 ( $1.3-1.63\mu\text{m}$ ), (c) band 10 ( $0.44-0.63\mu\text{m}$ )., at which obvious difference exist in optical properties among schemes, to calculate upward flux, downward flux and its components and heating rate.

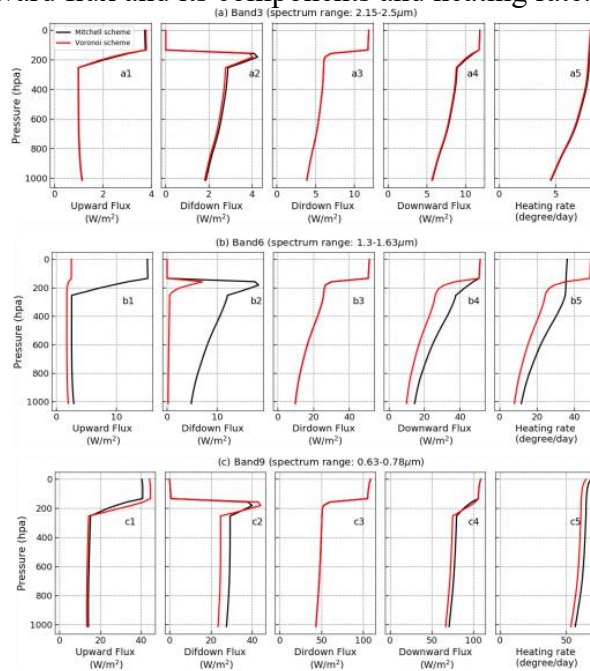


Figure 5. Vertical profiles of shortwave radiation flux (a1-c1) upward flux, (a2-c2) diffusedown flux, (a3-c3). directdown flux, (a4-c4). downward flux and (a5-c5).heating rate) at the band3, band6 and band9 for two schemes.

For Fig.5(b), as the height increases gradually into the cloud layer, the difference of upward flux between the schemes begins to increase, forming a large difference above the cloud top, reaching the maximum difference at the cloud top and then decreasing as the height grows. The downward diffuse flux is the opposite. From the whole atmosphere, the Voronoi scheme differs greatly from Mitchell schemes because it can be seen in Fig. 4 that the Voronoi scheme has a larger asymmetry factor than the Mitchell scheme; the asymmetry factor of the Voronoi scheme in the band3 ( $2.5-3.08\mu\text{m}$ ) is smaller than the Mitchell scheme. In Fig.5 (c), Voronoi scheme's downward shortwave flux is also significantly different from Mitchell schemes. The reason is as follows.

### 4.3. CESM run results

Vornoi scheme is applied in CESM CAM5.0 runs for climate effects analysis, thus Mitchell scheme is taken as a reference to compare with Voronoi schemes. Fugure7 shows zonal averages of SWCF and LWCF for Voronoi and Mitchell scheme, results show Vornoi scheme effects are strong in the tropics and in both mid latitude regions of the northern and southern hemispheres, where frequent storm-track happens (Fig.

7). The LW differences between Voronoi and Mitchell scheme are slightly small and are limited mostly to the tropics. Table 6 demonstrates the Voronoi scheme climate effects in CESM CAM 5.0 run and compares with evaluation results of three ice cloud scheme by Zhao et al., (2019). Note that TOA SW cloud forcing in Voronoi scheme matches more closely to observations compared with other three schemes. The global annual radiative effects by Voronoi scheme in CESM CAM5.0 run generally agrees with satellite observations.

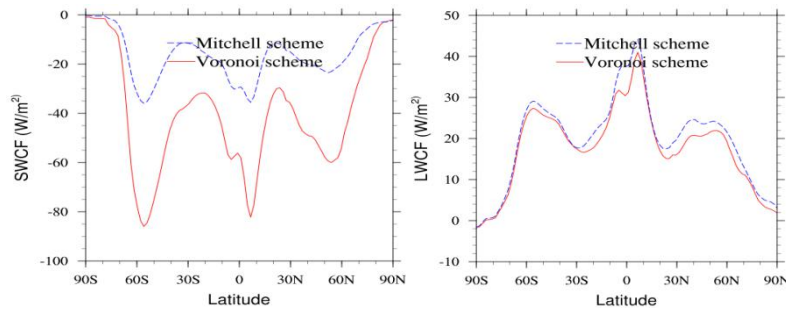


Figure 7. The zonal averages of TOA total SWCF (left) and LWCF (right), as simulated by CAM 5.1.

Table.6 Different ice cloud scheme CRF effects ( $Wm^{-2}$ ) from CESM CAM5.0 runs and satellite observations (Stephens et al., 2012) and CERES mean data.

	Baum-yang scheme	Mitchell scheme	Fu scheme	Voronoi scheme	CERES
TSCF	-56.55	-46.20	-54.66	-42.18	-42.29
TLCF	26.45	17.74	26.06	19.82	20.97

## 5. Conclusions

Current study assess the performance of ice cloud radiative properties description of Voronoi ice particle in a series of model simulations. Note that the downward direct flux is mainly up to cloud optical depth, which is depend on ice water path, extinction coefficients and ice effective radius. Downward and upward diffuse flux is largely dependent on the single scattering albedo and asymmetry factor. Significant difference of about up to 6-10.5% radiative effects can result from value bias of optical depths, and single-scattering albedos. In conclusion, Voronoi ice particle model has the advantages of ice cloud modeling capabilities in CESM1 CAM5 and possess the potential of applying into other global and zonal climate model. A tuning on ice cloud scheme in climate model may efficiently fix the discrepancy between simulation and observation.

## Reference

- Baran, A. J., and L. C.-Labonnote, 2006: On the reflection and polarisation properties of ice cloud. *J. Quant. Spectrosc. Radiat. Transfer*, 100, 41–54.
- Fu, Qiang & N. Liou, K. (1993). parametrization of the Radiative Properties of Cirrus Clouds. *Journal of the Atmospheric Sciences*. 50. 10.1175/1520-0469.
- Fu, Qiang. (1996). An Accurate parametrization of the Solar Radiative Properties of Cirrus Clouds for Climate Models. *Journal of Climate - J CLIMATE*. 9. 2058-2082. 10.1175/1520-0442.

- Heymsfield, A.J., Schmitt, C., Bansemer, A., 2013. Ice cloud particle size distributions and pressure-dependent terminal velocities from in situ observations at temperatures from 0° to -86 °C. *J. Atmos. Sci.* 70, 4123 – 4154.
- Ishimoto, H.; Masuda, K.; Mano, Y.; Orikasa, N.; Uchiyama, A. Irregularly shaped ice aggregates in optical modeling of convectively generated ice clouds. *J. Quant. Spectrosc. Radiat. Transf.* 2012 , 113, 632–643.
- Letu, H.; Ishimoto, H.; Riedi, J.; Nakajima, T.Y.; Labonnote, L.C.; Baran, A.J.; Nagao, T.M.; Sekiguchi, M. Investigation of ice particle habits to be used for ice cloud remote sensing for the GCOM-C satellite mission. *Atmos. Chem. Phys.* 2016, 16, 12287–12303.
- Mitchell, D.L., Chai, S.K., Liu, Y., Heymsfield, A.J., Dong, Y., 1996. Modeling cirrus clouds: part i. Treatment of bimodal size spectra and case study analysis. *J. Atmos. Sci.* 53, 2952–2966.
- Mitchell, D.L., Baran, A.J., Arnott, W.P., Schmitt, C., 2006. Testing and comparing the modified anomalous diffraction approximation. *J. Atmos. Sci.* 63, 2948–2962.
- Nakajima, T.Y., Ishida, H., Nagao, T.M., Hori, H., Letu, H., Higuchi, R., Tamaru, N., Imoto, N., Yamazaki, A., 2019. Theoretical basis of the algorithm and early phase results of the GCOM-C (Shikisai) SGLI cloud products. *Progress in Earth and Planetary Science.* <https://doi.org/10.1186/s40645-019-0295-9>.
- Yang, P., Bi, L., Baum, B. A., Liou, K. N., Kattawar, G. W., Mishchenko, M. I., and Cole, B., 2013: Spectrally consistent scattering, absorption, and polarization properties of atmospheric ice 10 crystals at wavelengths from 02 to 100 μm, *J. Atmos. Sci.*, 70, 330–347.
- Yi, B., Yang, P., Baum, B.A., L'Ecuyer, T., Oreopoulos, L., Mlawer, E.J., Heymsfield, A.J., Liou, K.-N., 2013. Influence of ice particle surface roughening on the global cloud radiative effect. *J. Atmos. Sci.* 70, 2794 – 2807.